

Specific Heat of the Dilute Ising Magnet $\text{LiHo}_x\text{Y}_{1-x}\text{F}_4$

J. A. Quilliam,^{1,2} C. G. A. Mugford,^{1,2} A. Gomez,³ S. W. Kycia,³ and J. B. Kycia^{1,2}

¹*Department of Physics and Astronomy, University of Waterloo, Waterloo, ON N2L 3G1, Canada*

²*Institute for Quantum Computing, University of Waterloo, Waterloo, ON N2L 3G1, Canada*

³*Department of Physics, University of Guelph, Guelph, ON N1G 2W1, Canada*

(Received 28 June 2006; published 18 January 2007)

We present specific heat data on three samples of the dilute Ising magnet $\text{LiHo}_x\text{Y}_{1-x}\text{F}_4$ with $x = 0.018$, 0.045, and 0.080. Previous measurements of the ac susceptibility of an $x = 0.045$ sample showed the Ho^{3+} moments to remain dynamic down to very low temperatures, and the specific heat was found to have unusually sharp features. In contrast, our measurements do not exhibit these sharp features in the specific heat and instead show a broad feature, for all three samples studied, which is qualitatively consistent with a spin glass state. Integrating C/T , however, reveals an increase in residual entropy with lower Ho concentration, consistent with recent Monte Carlo simulations showing a lack of spin glass transition for low x .

DOI: 10.1103/PhysRevLett.98.037203

PACS numbers: 75.10.Jm, 75.40.Cx, 75.50.Lk

Extensive work has previously been done to understand the spin glass transition found in disordered magnetic systems [1] and changes in behavior as the concentration of magnetic moments is reduced [2]. The material $\text{LiHo}_x\text{Y}_{1-x}\text{F}_4$ is a nearly perfect example of a dilute, dipolar-coupled Ising magnet and is therefore an ideal system for experimentally testing theories of simple, interacting spin models. Despite the apparent simplicity of this system's underlying model, however, a series of surprising results and fascinating effects has emerged from the material's rich phase diagram, especially at low concentrations of magnetic Ho^{3+} ions [3–6].

At $x = 1$, the system has been found to order ferromagnetically with $T_c = 1.53$ K [7], but, below a certain amount of dilution ($x \simeq 0.25$), there is enough randomness and frustration (due to the angle-dependent dipolar interaction) that the system becomes a spin glass [3,8]. At $x = 0.045$, however, ac susceptibility experiments have shown the material to not freeze down to very low temperatures [3]. The absorption spectrum $\chi''(\omega)$ is observed to narrow with lower temperature where typically, in a spin glass, the absorption spectrum becomes wider as freezing of the moments leads to longer relaxation times [9]. Furthermore, at temperatures below 100 mK, there appears to be a gap in the absorption spectrum, and coherent, low frequency oscillations with lifetimes of up to 10 s are observed. These effects have been attributed to clusters of roughly 260 Ho ions acting as largely independent oscillators [4].

Since the dipolar coupling between the Ho moments is a long-range interaction, it has long been theoretically expected that there should be no finite concentration of moments (x) at which the ordering (or freezing) temperature of the system drops to zero [10]. The ac susceptibility experiments performed on the $x = 0.045$ sample, however, seem to contradict this theory as there is no sign of freezing

even down to 50 mK. Recent Monte Carlo simulations of dipolar-coupled Ising moments randomly placed on a cubic lattice do suggest that there is no spin glass transition for $x < x_c \simeq 0.20$, which could explain the unusual dynamics seen at $x = 0.045$ [11]. There is also evidence in recent μSR experiments on $\text{LiHo}_{0.045}\text{Y}_{0.955}\text{F}_4$ of spin dynamics persisting down to low temperatures [12].

This unique spin liquid or “antiglass” state has also exhibited unusually sharp features in its specific heat at around 110 and 300 mK. These features were qualitatively reproduced in numerical simulations using a model based on quantum entanglement of pairs of moments and a pairwise “decimation” procedure in which the sharp heat capacity features correspond to maxima in the distribution of dipolar couplings in the system [5]. This simulation was also able to reproduce a $T^{-0.75}$ behavior of the dc susceptibility which was observed experimentally. It is not known whether there is a relation between these heat capacity signatures and the anomalous dynamics observed by ac susceptibility.

In this Letter, we present specific heat data taken on three stoichiometries in this series: $x = 0.018$, 0.045, and 0.080; see Fig. 1. The samples studied are high quality single crystals grown with the Bridgman technique [13]. Crystalline quality was verified by high resolution diffraction on a fine focus Cu rotating anode generator equipped with a high resolution Ge (220) four-crystal monochromator and a Huber 4-circle diffractometer. The measurements revealed extremely sharp Bragg peaks ($\theta_{\text{FWHM}} < 0.015^\circ$) for all reflections, indicating high crystalline perfection. No twinning was observed. Extensive diffuse scattering measurements revealed no diffuse scattering near or away from the Bragg peaks or satellite peaks that could be associated with any disorder or short range ordering. Small ~ 100 μm fragments were taken from each sample, and crystallography data sets were measured using a molybdenum rotating anode, kappa diffractometer, and CCD

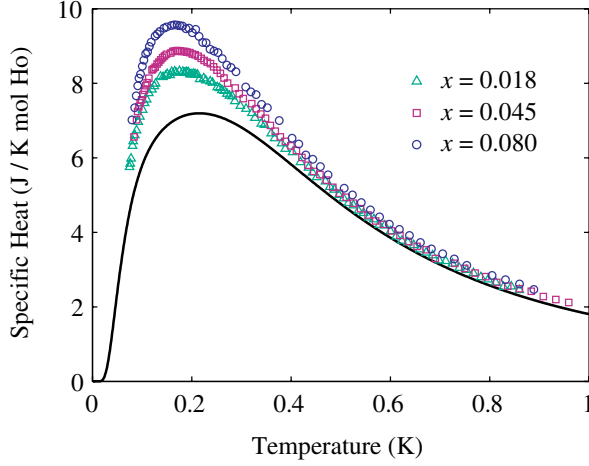


FIG. 1 (color online). Total measured specific heat for $x = 0.018$, $x = 0.045$, and $x = 0.080$. The solid line is the total noninteracting specific heat calculated by diagonalizing the crystal field and nuclear-hyperfine Hamiltonians.

area detector. All three data sets refined well with Ho substituting for Y in the expected tetragonal ($I4_1/a$) structure [14].

Measurements were performed using the quasiadiabatic method with a long time constant τ of relaxation. No substrate was used in these experiments, and the heater, thermometer, and weak link were glued directly onto the sample, which was suspended from very fine nylon threads. Using a substrate can lead to an underestimate of the heat capacity due to large thermal resistances between the sample and the substrate. The addendum was determined to be less than 0.1% of the sample's heat capacity. Samples were typically disks ~ 8 mm in diameter and ~ 1 mm thick.

A RuO_2 resistor (1 k Ω at 300 K) was used as a thermometer and a 10 k Ω metal-film resistor was used as a heater, both with thinned alumina substrates. Leads to the thermometer and heater were 6 μm diameter, ~ 5 mm, NbTi, superconducting wires with a thermal conductance of $K_{\text{NbTi}} \approx 8 \times 10^{-11}$ W/K at 1 K and at least a factor of 10 smaller at 100 mK. The thermal conductance from the thermometer and heater to the sample (K_{TS} and K_{HS} , respectively) was measured to be greater than 10^{-8} W/K at very low T (< 50 mK). The weak link connecting the sample to the dilution refrigerator mixing chamber was made from manganin wire and had a thermal conductance $K_{\text{WL}} \approx 1 \times 10^{-7}$ W/K at 100 mK. Calculations show that the temperature of the thermometer differs from that of the sample by less than 0.1%.

Thermometer resistance measurements were made with a LR-700 ac resistance bridge. The cell was contained in a copper radiation shield, and the cryostat was surrounded by a lead shield and two μ -metal shields to attenuate the external magnetic field. The thermometer resistance was consistent with a standard RuO_2 temperature dependence

[15] with no indication of self-heating in the range of our data. The RuO_2 thermometer was calibrated to a calibrated LakeShore Ge resistance thermometer and a cerium magnesium nitrate susceptibility thermometer.

Time constants on the order of several hours (at the lower temperatures) ensured that the sample was cooled very slowly and was therefore able to reach equilibrium. Cooling the sample even more slowly did not have a noticeable effect on the measured heat capacity. Temperature data were collected for up to 30 minutes on either side of the heat pulse, and the heat capacity is given by $C = \dot{Q}/\Delta T$, where ΔT is obtained through extrapolation to the midpoint of the pulse as is shown in Fig. 2(b).

For temperatures below 1 K, the specific heat of $\text{LiHo}_x\text{Y}_{1-x}\text{F}_4$ is dominated by a broad feature which arises from the $I = 7/2$ nuclear-spin degrees of freedom. The single-ion Hamiltonian (neglecting the dipolar and nearest-neighbor exchange interactions) is given by $\mathcal{H} = \mathcal{H}_{\text{CF}} + \mathcal{H}_{\text{HF}} + \mathcal{H}_{\text{Q}}$. The $4f$ electrons in Ho^{3+} are tightly bound, resulting in a significant nuclear-hyperfine interaction: $\mathcal{H}_{\text{HF}} = A\mathbf{I} \cdot \mathbf{J}$. \mathcal{H}_{Q} is the nuclear quadrupole interaction, and $\mathcal{H}_{\text{CF}} = \sum_{l,m} B_l^m O_l^m$ is the crystal field potential caused by surrounding ions (the O_l^m 's are Steven's operator equivalents).

If the crystal field Hamiltonian is diagonalized by itself, one obtains a ground-state, Ising doublet with an effective g factor of 13.8 and a next excited state at around 11 K. It is then, in some cases, safe to assume that the electronic moments are perfect Ising spins, and the specific heat can be expressed as the sum of an electronic contribution ΔC and a nuclear contribution

$$\frac{C_{\text{Nuclear}}}{R} = \left(\frac{\sum_m x_m e^{-x_m}}{\sum_m e^{-x_m}} \right)^2 - \frac{\sum_m x_m^2 e^{-x_m}}{\sum_m e^{-x_m}}, \quad (1)$$

where $x_m = -A_J g_{\text{eff}} m / 2g_J T + P m^2 / T$ and $m = -7/2, \dots, 7/2$. A fit of this form was successfully applied by Mennenga *et al.* to the specific heat of LiHoF_4 below the transition temperature [16]. We have made corrections to this form by diagonalizing the entire noninteracting Hamiltonian (a 136×136 matrix). We have used $A_J/k_B = 40.21$ mK, determined by EPR experiments on $\text{LiHo}_{0.02}\text{Y}_{0.98}\text{F}_4$ [17]. This is similar to the value $A_J/k_B = 39.8$ mK found for the pure material [18]. We have assumed an axially symmetric nuclear quadrupole interaction of strength $P = 1.7$ mK which was determined with EPR on free Ho^{3+} ions [19]. The crystal field parameters B_l^m were taken from Ref. [20]. The resulting single-ion specific heat is shown as the solid line in Fig. 1 and has been subtracted from the data to give ΔC in Fig. 3. This more detailed calculation of the noninteracting specific heat is lower than Eq. (1) by $\sim 4\%$ near the highest point of the curve.

As mentioned earlier, the validity of this subtraction depends on the assumption that the Ho^{3+} ions are perfect Ising moments. This is not entirely the case, as the nuclear-

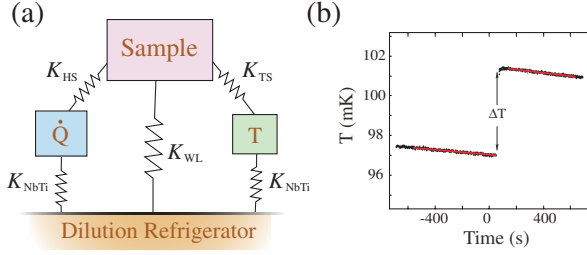


FIG. 2 (color online). (a) Diagram of relevant thermal links in experimental apparatus and (b) an example heat pulse showing linear fits and extrapolation to the midpoint of the pulse.

hyperfine interaction introduces mixing with the next excited states. Indeed, the nuclear-hyperfine interaction has been shown to strongly effect the magnetic ordering of the pure material in transverse field [20] and the diluted material in the spin glass regime [21]. Nevertheless, the total specific heat should approach this noninteracting specific heat at higher temperatures (close to 1 K). A small phonon contribution to the specific heat ($\propto T^3$) is also subtracted, estimated from the heat capacity of the pure material above 1 K [16].

The crystal supplier provided us with nominally 2%, 4.5%, and 8% concentrations of holmium. Assuming the correct nuclear-hyperfine component, however, the 2% sample appears to be closer to 1.8% as the remaining term ΔC should behave as T^{-2} at higher temperatures (close to 1 K). In this way, the 4.5% and 8% samples were confirmed to be the correct stoichiometry.

In all three samples, the remaining specific heat contribution ΔC is qualitatively similar and found to be a broad

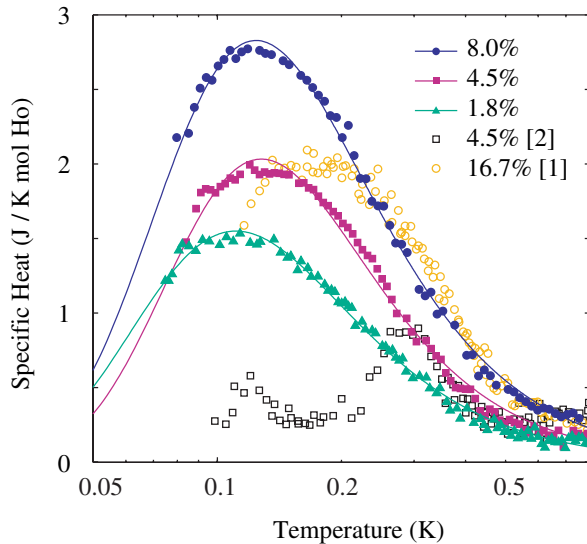


FIG. 3 (color online). Electronic moments' contribution to the specific heat (solid line from Fig. 1 subtracted) for $x = 0.018$, $x = 0.045$, and $x = 0.08$ from this work (solid symbols). Also $x = 0.045$ from Ghosh *et al.* [5] and $x = 0.167$ from Reich *et al.* [3] (open symbols). The solid lines are fits of the form of Eq. (2).

feature which is somewhat consistent with the heat capacity of a spin glass [22,23]. The specific heat of a spin glass is not expected to show a remarkable feature at the spin glass freezing transition as the critical exponent α is often negative, in the range -2 to -4 [24]. Instead of probing the actual freezing transition, the spin glass heat capacity is more indicative of excitations above the transition. The simplest situation is one excited energy state E_1 above the ground state having a degeneracy n with respect to the ground-state degeneracy. We can then apply fits of the form

$$\Delta C = C_0 \frac{n(E_1/k_B T)^2 e^{-E_1/k_B T}}{(1 - n e^{-E_1/k_B T})^2} \quad (2)$$

to the data. The resulting fitting parameters for these data and an $x = 0.167$ sample measured by Reich *et al.* [3] are shown in Table I. Clearly, the size of the specific heat features decreases with decreasing concentration x . The peak temperature of the curve, however, is very close in all three samples and does not appear to scale with the Curie temperature (xT_C).

Numerically integrating $\Delta C/T$ with respect to T gives the total amount of entropy released over the temperature range of these measurements. The total high-temperature entropy of an Ising magnet is $R \ln 2$, but there may be a residual ground-state entropy seen in doing this integral. Lower temperature data are required in order to confidently observe all the release of entropy in the system. We have extrapolated the data to 0 K, assuming a linear temperature dependence, before integrating $\Delta C/T$. Measurements at lower temperatures must be made in order to determine the temperature behavior of the specific heat below the maximum, but many past measurements have observed a linear temperature dependence in spin glasses [22,23] as described by the two-level system argument [25].

For the 8% sample, this integral reveals approximately all of the total expected entropy. In the 1.8% and 4.5% samples, however, our measurement observes a smaller percentage of $R \ln 2$: 56% and 70%, respectively, leaving a significant residual entropy S_0 . The residual entropy for each sample is also shown in Table I. These values may be

TABLE I. Fitting parameters for ΔC for $x = 0.018$, $x = 0.045$, and $x = 0.08$ from this work and data taken from Reich *et al.* ($x = 0.167$) [3]. The peak temperatures T_{peak} , the relative width of the specific heat curve $\text{FWHM}/T_{\text{max}}$ and the measured residual entropy S_0 (assuming a linear temperature dependence at low T) are also given.

Parameter	1.8%	4.5%	8.0%	16.7%
E_1/k_B (K)	0.26	0.32	0.29	0.46
n	0.85	1.43	0.86	1.89
T_{peak} (K)	0.11	0.13	0.12	0.17
$\text{FWHM}/T_{\text{peak}}$	1.7	1.6	1.7	1.5
S_0/R	0.31	0.21	0.00	0.18

compared to previous measurements for $x = 0.167$ where 75% of the entropy was measured (also assuming a linear temperature dependence below the peak) and $x = 0.045$ where only 15% of $R \ln 2$ was observed over the range of the measurement [3,5]. In the case of the 4.5% and 16.7% samples, S_0 is quite close to the value of $0.199R$ predicted by the Sherrington-Kirkpatrick model of a spin glass [26].

The Monte Carlo simulations of Snider and Yu on a dilute dipolar-coupled Ising system predict 0 residual entropy at $x = 0.20$ [11]. For $x < 0.20$, they see no spin glass ordering and an increasing S_0 with decreasing x as a larger number of degenerate ground states are available. This is the same trend observed in our data, though experimentally, the magnitude of the residual entropy is much larger. In the real system, the point at which spin glass ordering ceases must be lower than $x = 0.167$ as this has been observed to be a spin glass [3] and may be closer to $x = 0.080$, at which point we have observed the release of nearly all of the expected entropy.

The relative broadness of the observed features may be parametrized by the full width at half maximum (FWHM) divided by the peak temperature T_{\max} . The three samples studied here give values around 1.7 (see Table I). This parameter is approximately 1.2 in AuFe [27] and 1.5 in $\text{Eu}_x\text{Sr}_{1-x}\text{S}$, for example [23]. Typically, the maximum in the specific heat of spin glasses is found to be approximately 20% higher than the spin glass transition temperature which is determined by ac susceptibility experiments [1]. If this rule of thumb were to apply here, it would give spin glass transition temperatures of 90–100 mK for these three samples.

We have measured the specific heat of three samples at and around a concentration of 4.5% holmium, and our measurements do not exhibit the sharp features that were seen previously [3,5]. The data sets agree well until ~ 300 mK, which indicates that there is no error in stoichiometry. Below this point, however, there is a significant discrepancy. Our data, therefore, also do not support the theoretical model presented by Ghosh *et al.* [5]. We have taken great care to rule out any experimental errors such as decoupling of the thermometer from the sample. Recent thermal conductivity measurements of $\text{LiHo}_{0.04}\text{Y}_{0.96}\text{F}_4$ also do not show any remarkable features at 110 and 300 mK [28]. In some systems which have $\chi \sim T^{-\alpha}$, the specific heat also shows a simple power law behavior with a related exponent [29]. It would be interesting to measure $C(T)$ to lower temperatures to look for such an effect.

The specific heat data are consistent with a spin glass in that the observed feature is a broad maximum with no pronounced anomalies. However, it is not clear how the unusual spin liquid or antiglass state observed with ac susceptibility [3,5] should manifest itself in specific heat measurements. Based on the numerical simulations of Snider and Yu [11], the measured increase in entropy may indicate that the system is no longer a spin glass

below $x \approx 0.08$ and is instead a spin liquid with many accessible nearly degenerate ground states.

We have benefited greatly from discussions with M. J. P. Gingras and G. M. Luke. Also thanks to N. F. Heinig, S. Meng, L. Lettress, and N. Persaud. Thanks to J. F. Britten for a part of the x-ray characterization. Funding for this research was provided by NSERC, CFI, MMO, and Research Corporation grants.

-
- [1] K. Binder and A. P. Young, *Rev. Mod. Phys.* **58**, 801 (1986).
 - [2] H. Maletta and W. Felsch, *Phys. Rev. B* **20**, 1245 (1979); J. Kotzler and G. Eiselt, *Phys. Rev. B* **25**, 3207 (1982).
 - [3] D. H. Reich *et al.*, *Phys. Rev. B* **42**, 4631 (1990).
 - [4] S. Ghosh *et al.*, *Science* **296**, 2195 (2002).
 - [5] S. Ghosh *et al.*, *Nature (London)* **425**, 48 (2003).
 - [6] J. Brooke *et al.*, *Science* **284**, 779 (1999); J. Brooke, T. F. Rosenbaum, and G. Aeppli, *Nature (London)* **413**, 610 (2001).
 - [7] D. Bitko, T. F. Rosenbaum, and G. Aeppli, *Phys. Rev. Lett.* **77**, 940 (1996).
 - [8] W. Wu *et al.*, *Phys. Rev. Lett.* **67**, 2076 (1991); W. Wu, D. Bitko, T. F. Rosenbaum, and G. Aeppli, *Phys. Rev. Lett.* **71**, 1919 (1993).
 - [9] D. Hüser *et al.*, *Phys. Rev. B* **27**, 3100 (1983); C. C. Paulsen, S. J. Williamson, and H. Maletta, *Phys. Rev. Lett.* **59**, 128 (1987).
 - [10] M. J. Stephen and A. Aharony, *J. Phys. C* **14**, 1665 (1981).
 - [11] J. Snider and C. C. Yu, *Phys. Rev. B* **72**, 214203 (2005).
 - [12] J. Rodriguez *et al.*, *Physica (Amsterdam)* **374B**, 13 (2006).
 - [13] Purchased from TYDEX, J.S.Co., St. Petersburg, Russia.
 - [14] E. Garcia and R. R. Ryan, *Acta Crystallogr. Sect. C* **49**, 2053 (1993).
 - [15] F. Pobell, *Matter and Methods at Low Temperatures* (Springer-Verlag, Berlin, 1992).
 - [16] G. Mennenga, L. de Jongh, and W. Huiskamp, *J. Magn. Mater.* **44**, 59 (1984).
 - [17] J. Magariño *et al.*, *Phys. Rev. B* **13**, 2805 (1976).
 - [18] J. Magariño *et al.*, *Phys. Rev. B* **21**, 18 (1980).
 - [19] A. Abragam and B. Bleaney, *Electron Paramagnetic Resonance of Transition Ions* (Clarendon, Oxford, 1970).
 - [20] P. B. Chakraborty *et al.*, *Phys. Rev. B* **70**, 144411 (2004).
 - [21] M. Schechter and P. C. E. Stamp, *Phys. Rev. Lett.* **95**, 267208 (2005).
 - [22] L. E. Wenger and P. H. Keesom, *Phys. Rev. B* **13**, 4053 (1976); G. J. Nieuwenhuys *et al.*, *Physica (Utrecht)* **69**, 119 (1973).
 - [23] D. Meschede *et al.*, *Phys. Rev. Lett.* **44**, 102 (1980).
 - [24] K. H. Fischer and J. A. Hertz, *Spin Glasses* (Cambridge University Press, Cambridge, England, 1991).
 - [25] P. W. Anderson, B. I. Halperin, and C. M. Varma, *Philos. Mag.* **25**, 1 (1972).
 - [26] F. Tanaka, *J. Phys. C* **13**, L951 (1980).
 - [27] D. L. Martin, *Phys. Rev. B* **21**, 1902 (1980).
 - [28] J. Nikkel and B. Ellman, *cond-mat/0504269*.
 - [29] M. Brunner *et al.*, *Physica (Amsterdam)* **233B**, 37 (1997).